International Journal of Pharmaceutics 684 (2025) 126132

Contents lists available at ScienceDirect

International Journal of Pharmaceutics

journal homepage: www.elsevier.com/locate/ijpharm

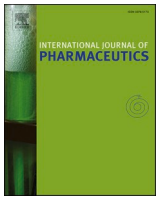

Simulation-based content uniformity engineering for drug development and manufacturing

Kevin T. Chu [a,1], Remus Osan [b,1], Nicole Tin [b], Somdatta Bhattacharya [b], Chiajen Lai [b,*]

[a] Velexi Corporation, Burlingame, CA 94010, USA
[b] Gilead Sciences, Foster City, CA 94404, USA

ARTICLE INFO

Keywords:
Content Uniformity
Monte Carlo Simulation
Particle Size Distribution

ABSTRACT

Stochastic models and Monte Carlo (MC) simulations of content uniformity (CU) are powerful tools for assessing CU risk without extensive experimental effort. However, simulations are valuable only if they are accurate, used appropriately, and embedded within natural operational workflows. Toward these ends, we first analyze a stochastic model of tablet formation to develop simple quantitative characterizations of dose regimes based on the active pharmaceutical ingredient (API) particle size distribution (PSD) that provide early guidance on CU risk. Second, we study a MC simulation of the stochastic tablet formation model to validate the importance of selecting upper particle size cutoff diameters used in simulation based on manufacturing processes including a margin of safety. Finally, we demonstrate simulation-based PSD engineering and CU risk assessment tools for process chemists and formulators designed to fit into common workflows, such as early-stage guidance for PSD targets, predicting USP < 905 > pass rates and statistics, and exploring the API PSD parameters and dose strengths where CU risk is low.

1. Introduction

Determining the appropriate dosage for a pharmaceutical product is a complex process involving numerous factors, with one of the most critical being the balance of pharmacological benefits and risks (Zheng, 2009). This is especially important for highly potent compounds, as high potency typically translates to high toxicity. Therefore, researchers must identify an optimal dosage to achieve the desired efficacy without compromising patient safety. For these highly potent (thus requiring low dose) drugs, stringent control measures must be established in the manufacturing process to ensure the drug product's content uniformity (CU) – under-dosing renders the drug ineffective while over-dosing increases the risks of adverse effects (Park et al., 2013).

The active pharmaceutical ingredient (API) particle size distribution (PSD) is the most critical quality attributes impacting the uniformity of low-dose drugs (Zheng, 2009). Intuitively, small particles are required to enhance the homogeneity of drug product intermediates (e.g., blends). In early development, where drug substance supply is limited, scientists may opt for the "as-small-as-possible particle size" mindset, leaving micronization as the primary option. However, the aggressive mechanical stresses involved in micronization often results in undesirable powder properties such as irregular shape (Rhodes and Seville, 2024), agglomeration (Saravanan et al., 2021), high surface energy (Gamble et al., 2012; Olusanmi et al., 2014; Saravanan et al., 2021), high cohesiveness (Schulze, 2021), electrostatics (Lachiver et al., 2006), and blending issues (Olusanmi et al., 2014). Defining a particle size specification with performance-oriented goals (e.g., dissolution kinetics, CU) while also considering processibility and manufacturing robustness is a crucial element of pharmaceutical development. Historically, this has been practiced empirically using experiments that offer clear readouts (pass/fail CU) in a quantized manner. However, the lengthy unit operations and the high material requirements to enable a formulation scale-up make it an impractical exercise to thoroughly verify the appropriateness of the specification across a range of processing parameters. Instead, a predictive tool to simulate the tablet-making process would enable (1) continuous statistics and (2) virtual experimentation of numerous "what-if" scenarios. The modeling approach is an effective alternative to defining API specifications required to meet the CU criteria.

Several publications have established the theoretical foundations for stochastic CU models and continuously improved these models through evolving mathematics and a changing regulatory landscape. Johnson

* Corresponding author at: Gilead Sciences, Foster City, CA 94404, USA.
E-mail address: chiajen.lai@gilead.com (C. Lai).
[1] Equal contribution.

https://doi.org/10.1016/j.ijpharm.2025.126132
Received 24 July 2025; Received in revised form 26 August 2025; Accepted 30 August 2025
Available online 1 September 2025

(Johnson, 1972, Johnson, 1975) derived and validated the correlation between drug content variation and API PSD based on a random retrieving model that involves ideally mixed particles that follow Poisson statistics. Johnson's model can predict the CU of any arbitrary PSD; however, the practical implementation proves to be laborious due to summation across many particle-size bins. Yalkowsky and Bolton (Yalkowsky and Bolton, 1990) addressed this challenge by introducing a major assumption, that of log-normal PSD, which streamlined the mathematical treatment. This method allows one to use the predicted CU variation to calculate the probability of passing USP criteria (USP < 28 >). While the Yalkowsky-Bolton method was based on less commonly used PSD descriptors (arithmetic mean diameter and arithmetic standard deviation), their approach created the possibility of setting particle size specifications for a given dosage in an *a priori* manner. Zhang and Johnson (Zhang and Johnson, 1997) later demonstrated similar predictions of the potency distribution based on computational tools and complemented by experimental verification.

The equivalence of the Johnson and Yalkowsky-Bolton equations under the log-normal PSD assumption was confirmed by Rohrs et al. (Rohrs et al., 2006). The CU acceptance criteria at the point of Rohrs' publication were based on a procedure compatible with a statistical model involving relatively simple analytical terms. Under the USP < 28 > framework, the authors derived approximate closed-form expressions for the CU acceptance probability in terms of the relative standard deviation (RSD) of the potency distribution. These expressions entail straightforward probability functions and conditional probabilities. The nomograph presented by Rohrs et al. (Rohrs et al., 2006) provides easy access to gauge the probability of passing the CU test with only three formulation-related variables – the target dose (D), volume-based particle size (d_{50} or d_{90}), and geometric standard deviation of the PSD (σ_g).

Despite its simplicity, the analytical formulas derived by Rohrs et al. (Rohrs et al., 2006) have limited applicability in practice because they require the following assumptions: (1) normality of the potency distribution (2) a log-normal API PSD, and (3) statistical independence of the RSD of a batch of tablets and the event that all the tablets in that batch fall within a particular range.

As observed by Rohrs et al. (Rohrs et al., 2006), the first assumption breaks down in the low dose regime (relative to the average potency), and the second assumption is simply not representative of real-world API PSD (Olusanmi et al., 2014). Milling (Seibert et al., 2019) is known to broaden the PSD due to a wide spectrum of breakage forces that often lead to multimodal and asymmetric distributions. A subsequent sieving step to remove large particles or agglomerates could further truncate and complicate the PSD. The last assumption, which is implicit in the derivations, is mathematically invalid because the potency of dose strength in a sample affects the RSD of the sample. A more rigorous first-principles model that evaluated the contribution of individual particle-size bins on dose uniformity was proposed by Hilden et al. (Hilden et al., 2012). The authors' derivation indicated that D [6,3],[2] an uncommon yet readily accessible particle size statistic from light scattering measurements, elucidates the relationship between unit dose RSD and the API PSD through

$$\mathrm{RSD} = \sqrt{\frac{\pi}{6} D[6,3]^3} \bullet \sqrt{\frac{\rho}{Dose}}$$

This generalization makes D [6,3] a suitable predictor of unit dosage uniformity without any PSD assumptions (i.e., the PSD could be multimodal), thus addressing a limitation of Rohrs' model which mandates a log-normal PSD (Rohrs et al., 2006).

Table 1
Criteria for USP < 905 > Uniformity of Dosage Units.

Acceptance Criteria Stage 1 (n = 10)	Stage 2 (n = 30)
$AV_{stage1} \le L_1$	$AV_{stage1} > L_1$ $AV_{stage2} \le L_1$Must meet: $(1–0.01 \cdot L_2) \cdot M \le X_i \le (1 + 0.01 \cdot L_2) \cdot M$
Acceptance Value (AV)	
$AV = \lvert M - \bar{X} \rvert + ks$	
Parameter Details	
M (Reference Value)	
If 98.5 % ≤ $\bar{X}$ ≤ 101.5 %	Then M = $\bar{X}$ (AV = ks)
If $\bar{X}$ < 98.5 %	Then M = 98.5 % (AV = 98.5 % − $\bar{X}$ + ks)
If $\bar{X}$ > 101.5 %	Then M = 101.5 % (AV = $\bar{X}$ − 101.5 % + ks)
$\bar{X}$ (Mean of individual content)	$\bar{X} = \frac{1}{n}\sum_{i=1}^{n} X_i$
s (Sample standard deviation)	$s = \left[\frac{\sum_{i=1}^{n}(x_i - \bar{X})^2}{n-1}\right]^{\frac{1}{2}}$
k (Acceptability constant)	
If n = 10	Then k = 2.4
If n = 30	Then k = 2.0
n (Number of units in a sample)	
L_1 (Maximum allowed acceptance value) = 15 (unless otherwise specified)	
L_2 (Maximum allowed range for deviation = 25 (unless otherwise specified)	
X_i (Individual contents of the unit dosage tested)	

[Δ]The target content per dosage unit is assumed to be identical to the manufacturer's label claim.

The harmonization of US Pharmacopeial < 905 > with the European and Japanese Pharmacopoeia on the Uniformity of Dosage Units, which commenced in 2008 and was updated as recently as 2023 (USP, 2023), called for the use of a new system of parameters as the criteria for a two-stage assessment process. The current USP < 905 > can be briefly summarized in Table 1[Δ] (Huang and Ku, 2010a; Hudson-Curtis and Novick, 2016; USP, 2023).

Implementing USP < 905 > requires several variables whose values are determined through a decision-tree process (e.g., M, k, L_1, L_2). The other implication of the replacement of USP < 28 > by the more logically complex USP < 905 > is that simple analytical treatment such as Rohrs et al. (Rohrs et al., 2006) and the algebraic manipulation of the probability functions are no longer practical. Instead, simulations by computational methods for predicting CU acceptance probabilities from formulation parameters are more appropriate because they can handle the high complexity of the logic and impose fewer assumptions.

Huang and Ku proposed an innovative approach based on the Monte Carlo (MC) algorithm (Huang and Ku, 2010a) – a versatile computational technique adopted by many scientific fields, including pharmaceuticals (Chang, 2010; Martins et al., 2024). MC uses repeated random sampling to estimate the probability distribution and statistics of variables in processes that are not (1) easy to predict deterministically or (2) inherently depend on random variables. By generating a large number of random events and observing the distribution of the results, scientists can estimate the likelihood of various outcome scenarios. Huang and Ku (Huang and Ku, 2010a) used this methodology and first derived analytically the skewness of potency distribution (α_3) and coefficient of variation (C_v) functions based on random retrieving theory and Poisson distribution of API particles in the dosage unit. Their derivation revealed a unique sensitivity of α_3 and C_v to the dose (both scale as dose$^{-1/2}$), which was vetted through experimental data (Rohrs et al., 2006), and an inherent divergence from normality due to positive skewness. The authors then applied the MC method to simulate the full potency distribution, showing remarkable agreement with theoretical derivation. Their investigation proved the breakdown of the normality assumption, which gives an overly forgiving estimate of the CU pass rate. The simulation results warrant a more stringent control of the PSD and dosage variation to accommodate the anisotropy of the data distribution.

[2] For particle size distribution by laser light scattering (LLS) method, the calculation of the mean diameter based on different weighing can be generalized as:$D[a,b] = \frac{\sum n \bullet d^a}{\sum n \bullet d^b}$. where n is number of particles and d is diameter. As an example, a commonly used property for particle size characterization is D [4,3], the volume-weighted (De Brouckere) mean diameter.

A nomograph of the median particle size (d_{50}) vs. the dose limit (D (mg)/ρ*) covering a range of typical particle size standard deviation (σ) was presented by the authors to map out the target PSD that affords a 99 % passing rate under USP < 905 > . The nomograph is a convenient and powerful tool that synergizes with contemporary development strategy (e.g., quality by design (Yu, 2008; Lionberger, 2008) and predictive tools (Wang et al., 2019; Parikh et al., 2021)) advocated by the regulatory authorities. Moreover, an extension of Huang and Ku's model (Huang and Ku, 2010b) that specifically addressed the asymmetry of the PSD, a situation most representative of a real API after the milling operation, further reveals valuable insight from the simulations. For mathematical simplicity, the authors adopted a log-skew-normal (L-S-N) distribution proposed by Azzalini (Azzalini 1985, Azzalini 1986) and defined an asymmetry parameter ε as

$$\varepsilon = \frac{\ln d_{90} - \ln d_{50}}{\ln d_{50} - \ln d_{10}}$$

Including the asymmetry parameter (ε) as an extra variable in the MC simulation changed the topology of the nomograph. The authors found that the removal of large-size particles by sieving (or equivalently, implementing a truncation in the MC simulation) also dramatically changes the d_{50} vs. D/ρ landscape. The exploration of various scenarios via modeling effectively allowed the scientists to assess the risk level of over or under-potency of low-dosage drugs.

Huang and Ku's work provides a theoretical foundation and a framework to quantitatively connect the CU acceptance outcome with formulation parameters and API quality attributes (e.g., dosage, d_{90}/d_{50}, asymmetry of PSD). The key merit of the MC approach is that (1) the numerical simulation is appliable to any arbitrary PSDs (including empirical, multimodal distributions) (2) flexibility to accommodate the logic of USP < 905> (or any future revisions) and inclusion of other descriptors (e.g., ε) to better reflect reality. Most importantly, the constraints encountered in previous studies, such as assuming log-normal PSD and normality of potency distribution, are easy to relax in a computer algorithm.

In this contribution, we build on and complement Huang and Ku's ideas in three main areas. First, we provide a more quantitative approach for assessing whether CU risk is present *prior to simulation*. Second, we more carefully evaluate the impact of parameters (e.g., PSD upper cutoff diameter) on simulation accuracy and CU risk predictions. Finally, we demonstrate how to use the simulation in the context of PSD control during crystallization and post-isolation operations (e.g., milling, sieving). More specifically, we identify critical engineering principles when using MC simulations for API and formulation process development.

- We define simple and intuitive quantitative classifications of dose regimes based on quantities readily computed from the particle size distribution and the target dose strength (Section 2). These dose regimes enable early detection of potential CU failure risks and provide guidance on process design during API PSD engineering. Also, the characterization of dose regimes (e.g., large tablet dose variance vs. skewed tablet dose distribution) into different classes (even qualitatively) appears to be novel.
- We analyze and validate existing MC simulation algorithms for CU using computational convergence studies (Section 3). These studies yield critical understanding about the impact of the PSD upper cutoff diameter on CU predictions. There are many mathematical and numerical details in this section, which are part of our main contributions.
- We develop and assess simulation design elements and principles that support API particle size engineering (Section 4). Using the insights gained from computational experiments and comparison of simulation predictions with experimental data, we propose strategies for incorporating MC simulations into tablet formulation and API manufacturing workflows. We also suggest engineering strategies to mitigate risks associated with the deviations between simulation and experiment.

2. Theoretical foundations

2.1. Tablet formation model

Following the standard approach (Rohrs et al., 2006; Yalkowsky and Bolton, 1990; Huang and Ku, 2010a), we model tablet formation as a stochastic process (Pinsky and Karlin, 2011). The dose strength of a tablet is the sum of the amounts of API contained in the particles that are used to form the tablet, where both the number of particles and the amount of API contained in each particle are random variables. This stochastic model provides the foundation for analysis of the dose distribution and study of derivative quantities, such as the CU pass rate.

Following Huang and Ku (Huang and Ku, 2010a), the dose strength contained in a tablet can be expressed as

$$D = \sum_{i=1}^{n} w_i \tag{1}$$

where D is the tablet dose strength, each w_i is a random variable equal to the amount of API in the i-th particle, and n is a random variable equal to the number of particles contained in the tablet. Assuming that all particles are spherical[3] and have the same API density, the dose can be written in terms of particle diameters d_i

$$D = \sum_{i=1}^{n} \frac{\pi \rho d_i^3}{6} \tag{2}$$

where ρ is the API density (true density based on crystal structure). Expressing D in this form shows that the dose distribution is completely determined by (1) the API particle size distribution (PSD) and (2) the distribution of the number of particles in each tablet.

The API PSD is typically obtained from experimental measurements such as light-scattering methods (Gamble et al., 2019). For API produced via a crystallization process, the PSD is often observed to resemble a log-normal distribution (or a truncated log-normal distribution if a sieving step is implemented to remove large particles). The distribution of the number of particles n in a tablet is not readily observable. However, under the assumptions that (1) API particles do not form strong agglomerates (Huang and Ku, 2010a) and (2) the number of particles available to form each tablet is much larger than the number of particles in a single tablet, the law of rare events suggests that it is reasonable to approximate by a Poisson random variable (Pinsky and Karlin, 2011):

$$P[n = k] = \frac{\lambda^k e^{-\lambda}}{k!}, \tag{3}$$

where $P[n = k]$ is the probability that the number of particles n is equal to k, and λ is the expected value of the Poisson distribution. In the context of tablet formation, the parameter λ of the Poisson distribution is set so that the average dose is equal to the target dose strength D_0:

$$D_0 = \langle D \rangle = \langle n \rangle \langle w \rangle = \lambda \langle w \rangle. \tag{4}$$

In other words, we set λ equal to $D_0/\langle w \rangle$, where $\langle w \rangle$, the average amount of API contained in a single API particle, can be computed from the PSD.

2.2. Analytical formulas for moments of the dose distribution

Within the framework of the stochastic tablet formation model, it is straightforward to derive analytical formulas for several of the moments of the dose distribution. These formulas are useful for providing a

[3] Spherical particle is an essential assumption for the development of this model for mathematical simplicity. It should be noted that deviation from the spherical shape inevitably leads to variance of model predictions.

theoretical foundation for assessing content uniformity risks (Section 2.3), validating simulation methodology (Section 3.2), and testing software implementations.

Following Huang and Ku, we express the dose distribution in terms of the moments of the particle size and particle count distributions (Huang and Ku, 2010a):

$$Var(D) = \langle (D - D_0)^2 \rangle = \langle n \rangle Var(w) + Var(n) \langle w \rangle^2 \tag{5a}$$

$$\mu_3(D) = \langle (D - D_0)^3 \rangle = \langle n \rangle \mu_3(w) + 3 \langle w \rangle Var(w) Var(n) + \mu_3(n) \langle w \rangle^3 \tag{5b}$$

where $Var(X)$ and $\mu_3(X)$ are the variance and third central moment of the random variable X, respectively. Under the Poisson approximation for the particle count distribution, these expressions simplify to

$$Var(D) = \lambda \langle w^2 \rangle \tag{6a}$$

$$\mu_3(D) = \lambda \langle w^3 \rangle \tag{6b}$$

because $\lambda = \langle n \rangle = Var(n) = \mu_3(n)$ when n is a Poisson random variable with parameter λ.

Using these formulas to compute the coefficient of variation C_v and skewness α_3 leads to the theoretical observation that both quantities are inversely proportional to the square root of the target dose strength (Huang and Ku, 2010a):

$$C_v = \frac{Var(D)^{\frac{1}{2}}}{\langle D \rangle} = \frac{1}{\sqrt{D_0}} \left(\frac{\langle w^2 \rangle}{\langle w \rangle} \right)^{\frac{1}{2}} \tag{7a}$$

$$\alpha_3 = \frac{\mu_3(D)}{Var(D)^{\frac{3}{2}}} = \frac{1}{\sqrt{D_0}} \left(\frac{\langle w \rangle^{\frac{1}{2}} \langle w^3 \rangle}{\langle w^2 \rangle^{\frac{3}{2}}} \right) \tag{7b}$$

2.3. Dose regimes

Using the analytical formulas for the moments of the dose distribution, we can define dose regimes with distinct characteristics. These dose regimes make it possible to assess content uniformity risk and identify what types of failures to expect based only on the API PSD (either empirical or theoretical) – shifting CU risk management earlier in the development cycle (from both laboratory and simulation perspectives).

2.3.1. Dose variance regimes

One component of the USP < 905 > protocol is an estimate of the relative standard deviation[4] (RSD) for the dose distribution based on a sample of tablets from the manufactured batch. More specifically, a small multiple of the RSD is required to be less than a specified threshold. Thus, we can define dose variance regimes based on whether the expected RSD (or equivalently, coefficient of variation C_v) is sufficiently small to pass the most conservative USP < 905 > acceptance criteria. Combining equation (7a) with the logic for Stage 1 of USP < 905>, we expect that there may be risk passing USP < 905 > when target dose strengths are too small:

$$D_0 \lesssim \left(\frac{2.4}{0.15} \right)^2 \left(\frac{\langle w^2 \rangle}{\langle w \rangle} \right) \tag{8a}$$

where the constants 2.4 and 0.15 come from the values of k and L_1 in Stage 1 of USP < 905> (Table 1). When condition (8a) is satisfied, the ks term in the AV formula exceeds the L_1 limit for passing USP < 905 > during Stage 1.

Conversely, if the target dose strength is sufficiently large, there is little risk of USP < 905 > failure due to large dose variances:

$$D_0 \gg \left(\frac{2.4}{0.15} \right)^2 \left(\frac{\langle w^2 \rangle}{\langle w \rangle} \right) \tag{8b}$$

2.3.2. Dose skew regimes

For sufficiently high dose tablets (e.g., 200 mg), the dose distribution is well-approximated by a normal distribution – because the tablet dose is the sum of a large number of independent API amounts. At lower doses, the distribution is skewed (Huang and Ku, 2010a). When that happens, analytical approaches for assessing CU failure risk may not be sufficiently accurate in providing meaningful guidance, and simulation approaches are needed to determine CU failure risk accurately.

From equation (7b) for the skewness α_3 (which must equal 0 for Gaussian distributions), we expect that the dose distribution should deviate from normality (with high skew) at small dose strengths:

$$D_0 \lesssim \frac{\langle w \rangle \langle w^3 \rangle^2}{\langle w^2 \rangle^3} \tag{9a}$$

Conversely, if the target dose strength is sufficiently large, the dose distribution is expected to be close to normal:

$$D_0 \gg \frac{\langle w \rangle \langle w^3 \rangle^2}{\langle w^2 \rangle^3} \tag{9b}$$

2.3.3. Particle count characterization of target dose regimes

The dose regimes can also be characterized by the typical number of particles used to form a tablet (rather than the target dose D_0). Using $\langle v \rangle$ as a reference value for the particle volume, the number of particles needed to form a tablet is equal to

$$n^* = \frac{D_0}{\rho \langle v \rangle} \tag{10}$$

where ρ is the API density and v is the volume of a single particle. Combining this equation with the relationship between API mass and particle volume (i.e., $\langle w \rangle = \rho \langle v \rangle$) leads to a characterization of dose regimes expressed in terms of the number of particles per tablet. The relative dose variance C_v is expected to be large when

$$n^* \lesssim \left(\frac{2.4}{0.15} \right)^2 \left(\frac{\langle v^2 \rangle}{\langle v \rangle^2} \right) \tag{11}$$

and the probability distribution of the dose strength is expected to deviate from normality when

$$n^* \lesssim \frac{\langle v^3 \rangle^2}{\langle v^2 \rangle^3} \tag{12}$$

2.3.4. Example dose regime estimates for API having a log-normal PSD

As a concrete example of the dose regime assessment described above, consider an API with a density of 1 g/cm^3 and a log-normal PSD with parameters $d_{50} = 10\mu m$ and $d_{90} = 25\mu m$. For these values (assuming spherical particles), $\langle w \rangle \approx 5.2 \times 10^{-6} \frac{mg}{\mu m^3}$, $\langle w^2 \rangle \approx 2.7 \times 10^{-9} \left(\frac{mg}{\mu m^3} \right)^2$, and $\langle w^3 \rangle \approx 1.4 \times 10^{-10} \left(\frac{mg}{\mu m^3} \right)^3$. For this configuration, the C_v is expected to be large for D_0 values below $\approx 0.1mg$, and the dose distribution is expected to deviate from normality for D_0 values below $\approx 5mg$. These target dose strengths correspond to tablets with an average of $\approx$ 100 million particles and $\approx$ 5 billion particles, respectively.

Note that it is *not* the case that the target dose (D_0) where normality of the dose distribution breaks down is always greater than the D_0 where the variance of the dose distribution fails USP < 905 > . As an example of the reverse situation, consider an API with a density of 1.25 g/cm^3 and a log-normal PSD with parameters $d_{50} = 100\mu m$ and $d_{90} = 150\mu m$. For these parameters, $\langle w \rangle \approx 0.001 \frac{mg}{\mu m^3}$, $\langle w^2 \rangle \approx 2.6 \times 10^{-6} \left(\frac{mg}{\mu m^3} \right)^2$, and $\langle w^3 \rangle$

[4] RSD is defined as the ratio of the standard deviation to the mean of a random variable: σ/μ.

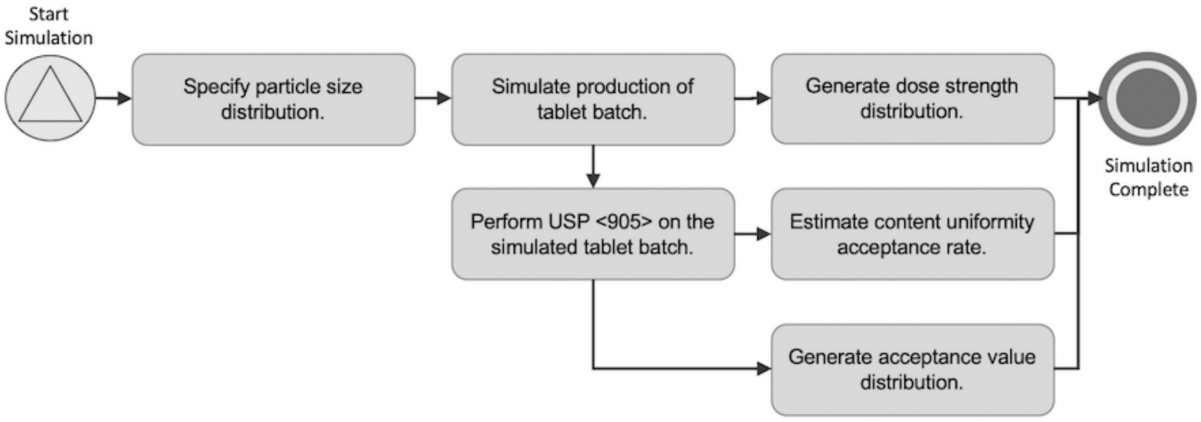

Fig. 1. Logical flow of a content uniformity simulation based on nested Monte Carlo algorithms. The first Monte Carlo simulation generates a tablet batch based on the tablet formation model. The second Monte Carlo algorithm simulates the USP < 905 > protocol to sample the distribution of USP < 905 > outcomes.

$\approx 1.6 \times 10^{-8} \left(\frac{mg}{\mu m^3}\right)^3$. For this configuration, the C_v is expected to be large for D_0 values below $\approx 0.6mg$ but the dose distribution is expected to deviate from normality for D_0 values below $\approx 0.015mg$.

These target dose strengths correspond to tablets formed with an average of ≈ 500 million particles and ≈ 10 million particles, respectively.

3. Monte Carlo simulations for content uniformity

In general, computational approaches are necessary to transform the tablet formation model described in Section 2 into practical information (e.g., content uniformity pass rates) because (1) empirical API PSDs are often not well-described by simple mathematical functions amenable to analytical manipulation, and (2) USP < 905>, the current CU test protocol, involves logic that complicates direct mathematical analysis.

3.1. Simulation algorithm

Following Huang and Ku (Huang and Ku, 2010a), we employ nested MC simulations: an inner MC simulation to generate a tablet batch that is used in an outer MC simulation to sample the distribution of USP < 905 > outcomes. The high-level flow of the simulation is illustrated in Fig. 1.

For the outer MC simulation, we repeatedly perform the USP < 905 > protocol to collect data on the outcomes (e.g., pass rate and distribution of acceptance values (AV)). For the inner MC simulation, tablet dose strengths are generated using the following multi-step process (Huang and Ku, 2010a).

1. **Specify the particle size distribution**. Suppose the PSD is well-approximated by a truncated log-normal distribution. In that case, we fit the empirical PSD data to a log-normal distribution and select truncation diameters that are consistent with the parameters of the API preparation process. In situations where the PSD is not well-approximated by a truncated log-normal distribution, we use the empirical PSD directly when simulating tablet formation.
2. **Construct a discrete approximation to the PSD**. Following Huang and Ku (Huang and Ku, 2010a), we discretize the PSD by constructing 100 diameter intervals and computing the probability of drawing a particle from each interval. If the PSD is specified by a truncated log-normal distribution, the diameter intervals are equally spaced in log-diameter space. Otherwise, the diameter intervals are defined by the instrument used to collect the empirical PSD.
3. **Compute volume fractions**. For each interval of the discretized PSD, we compute the approximate volume fraction of particles with diameters that fall within the interval. For this calculation, we make the following assumptions: (1) Particles are spherical. (2) The diameter of all particles in each interval is equal to the center of the interval.
4. **Generate the tablet batch**. Using the diameter intervals of the discrete approximation to the PSD and their volume fractions, we simulate the manufacturing of a batch of tablets. To generate a single tablet, we use the following procedure:

a. Compute the average number of particles to be selected from each diameter interval: $\left(\frac{D_0}{\rho V_k}\right) f_k$, where V_k is the volume of each API particle in the k-th diameter interval and f_k is the fraction of API particle volume contained in k-th diameter interval of the PSD.[5]
b. For each diameter interval, randomly select the number of particles to use from the interval. For the k-th bin, the Poisson distribution parameter λ_k is set to the average number of particles to select from the interval.
c. Compute the dose strength of the tablet by summing the amount of API contributed from each diameter interval.

3.2. Upper particle size cutoff strongly impacts simulation predictions

When developing simulations for theoretical API PSDs that extend to infinity (e.g., exponential and Gaussian distributions), we must truncate the probability distribution at a finite value that is "large enough" to minimize simulation artifacts. For PSDs with "fat tails" (e.g., log-normal distribution), the upper particle size cutoff strongly affects simulation predictions. The impact of the cutoff value has been previously observed (Huang and Ku, 2010b), but a quantitative analysis of simulation error appears to be absent from the literature. To improve our confidence that simulations yield meaningful results, we performed a numerical convergence study of errors in the moments of the dose distribution as a function of particle size cutoff (Section 3.2.1). Additionally, we systematically assessed the impact of the particle size cutoff on USP < 905 > pass rates (Section 3.2.2).

3.2.1. Accurate moments of dose distribution requires high upper particle size cutoff

For the numerical convergence study, we assume a log-normal distribution for the API PSD because analytical formulas are readily available for the moments of the log-normal distribution. The mathematical simplicity also allows the log-normal distribution to serve as a

[5] Here, k is an index on the diameter interval, *not* an index on the API particle that is incorporated into the tablet.

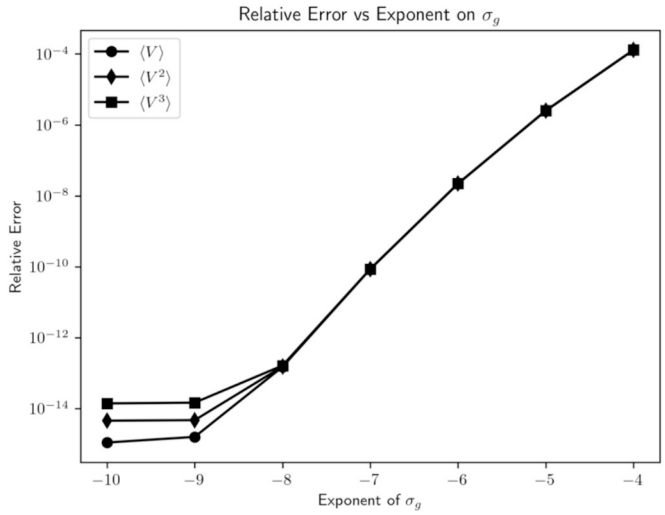

Fig. 2. The relative error of $\langle V \rangle$, $\langle V^2 \rangle$, and $\langle V^3 \rangle$ as a function of exponent on σ_g used to set the lower cutoff diameter. For these calculations, $d_{50} = 10\mu m$, $\sigma_g = 3$, and the upper cutoff diameter was set to $d_{50}\sigma_g^{20}$ (chosen large enough that the upper cutoff does not affect the error). Observe that the convergence rates for $\langle V \rangle$, $\langle V^2 \rangle$, and $\langle V^3 \rangle$ are all comparable.

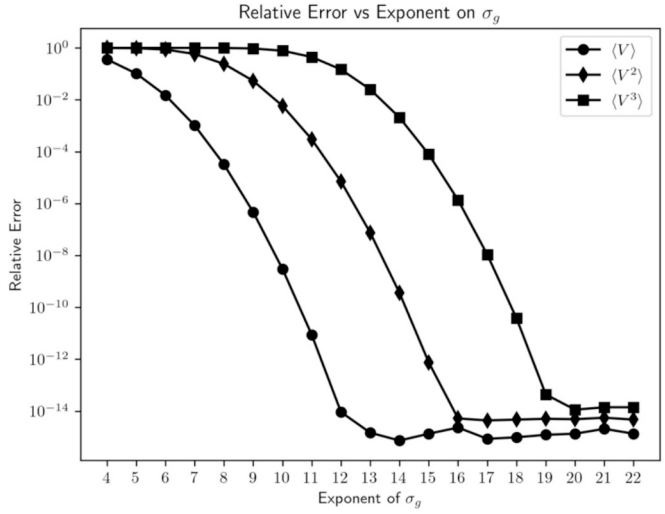

Fig. 3. The relative error of $\langle V \rangle$, $\langle V^2 \rangle$, and $\langle V^3 \rangle$ as a function of exponent on σ_g used to set the upper cutoff diameter. For these calculations, $d_{50} = 10\mu m$, $\sigma_g = 3$, and the lower cutoff diameter was set to $d_{50}\sigma_g^{-10}$ (chosen small enough that the lower cutoff does not affect the error). Observe that larger cutoffs are needed for the error of higher moments $\langle V \rangle$, $\langle V^2 \rangle$, and $\langle V^3 \rangle$ to converge. This behavior arises because the fat tail of the log-normal distribution results in large API particles making a significant contribution to the moments, with larger contributions for higher moments.

canonical example for understanding the impact of PSD with "fat tails."[6].

Equations (4), (5), and (6) show that the moments of the dose strength can be expressed as the expected value of powers of the API mass in a single API particle. Since API mass per particle is directly related to the particle volume, we designed our convergence study to investigate the dependence of the accuracy of numerical quadrature

[6] A probability distribution is said to have "fat tails" if a significant fraction of the probability is contained in the tails of the distribution.

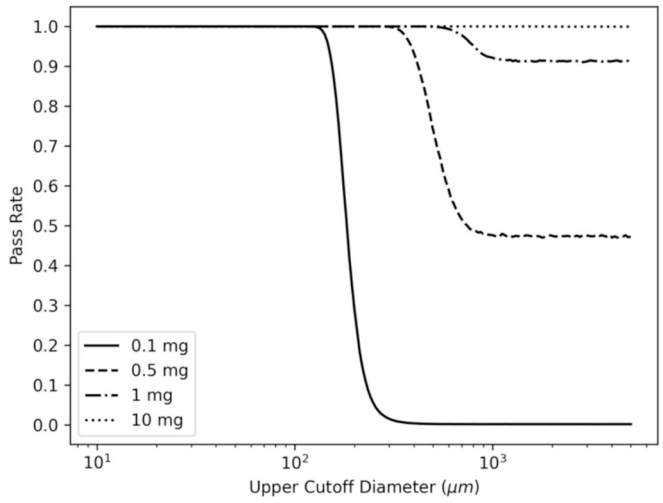

Fig. 4. The dose variance regimes are evident in the USP < 905 > pass rate curves (pass rate vs PSD upper cutoff diameter). In the low dose variance regime (dots), USP < 905 > has a high pass rate regardless of the upper cutoff diameters. In the medium dose variance regime (dot-dash and dash), the USP < 905 > pass rate is nonzero for all values of the upper cutoff diameter. In the high dose variance regime (solid), the USP < 905 > pass rate drops to zero for large upper cutoff diameters. These results were obtained for an API with density $1\ g/cm^3$ having a log-normal PSD distribution with $d_{50} = 20\mu m$ and $d_{90} = 50\mu m$.

formulas for $\langle V \rangle$, $\langle V^2 \rangle$, and $\langle V^3 \rangle$ on the particle size cutoff. For each of these quantities, we (1) varied both the lower and upper particle size cutoff diameters, (2) numerically evaluated the integral for the expectation value, (3) computed the relative error of the numerical calculations to the analytical formula for the expectation value, and (4) examined the dependence of the relative error on the lower or upper cutoff diameters. All numerical integration calculations were performed on a uniform grid with 1000 grid points in log-diameter space, which we confirmed produced numerical results accurate to be within machine precision in double-precision floating point arithmetic.

For the lower PSD cutoff diameter, the relative error decreases as the cutoff value approaches 0 and the $\langle V \rangle$, $\langle V^2 \rangle$, and $\langle V^3 \rangle$ values converge at comparable rates as the lower cutoff is decreased (Fig. 2). This result is not surprising because extremely small API particles do not significantly impact the expectation values.

For the upper cutoff diameter, the relative error decreases as the cutoff value approaches infinity (Fig. 3). Unlike the lower cutoff, the convergence rates for the upper cutoff are not the same for different moments of the volume – higher moments require larger cutoffs for a fixed level of accuracy. For the example shown in Fig. 3, a modest relative error of 10^{-4} for all three moments requires using an incredibly large upper cutoff of $\approx d_{50}\sigma_g^{15}$, which for the PSD parameters $d_{50} = 10\mu m$ and $\sigma_g = 3$ used in the study is equal to $143m$!

The main conclusion of the numerical convergence study is that to accurately compute the moments of the dose distribution *when the PSD* has a log-normal distribution (or any distribution with a "fat tail"), we must use very (unrealistically) large upper cutoff diameters. In practice, PSDs *never* have distributions that extend to infinity because the API manufacturing process typically involves steps that remove large particles. Therefore, whenever theoretical PSDs are used, they must always be appropriately truncated for simulation predictions to be practically meaningful.

3.2.2. USP < 905 > pass rate is highly sensitive to the upper particle size cutoff

The numerical convergence study above demonstrates that the upper cutoff diameter for a PSD with a log-normal distribution strongly affects

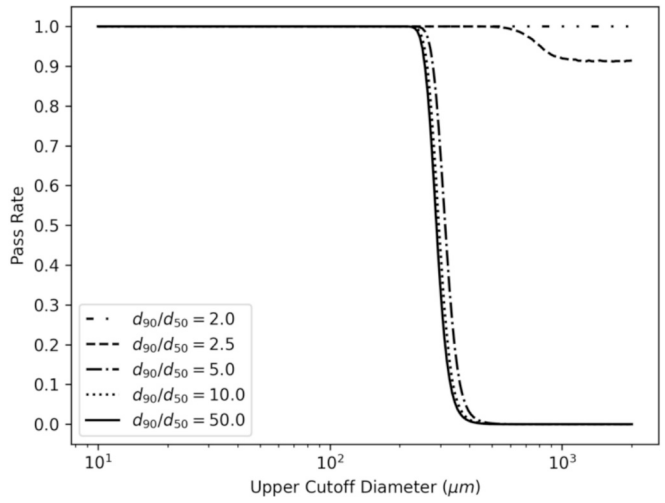

Fig. 5. API PSD variance dependence of the USP < 905 > pass rate curves (pass rate vs PSD upper cutoff diameter) for a fixed dose strength. In the low dose variance regime (dash and dot-dot dash), the USP < 905 > pass rate is nonzero even at large upper cutoff diameters. In the high dose variance regime (solid, dot and dot-dash), the USP < 905 > pass rate curve has a steep drop to zero as the upper cutoff diameter increases. Observe that the pass rate curves in the high dose variance regime are bunched together. These results were obtained for an API with density 1g/cm^3 having a log-normal PSD distribution with d_{50} = 20μm when the target dose strength is D_0 = 1 mg.

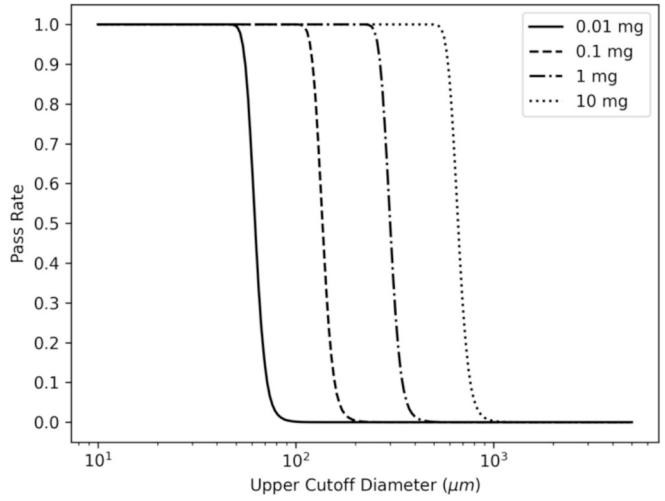

Fig. 6. Dose strength dependence of the USP < 905 > pass rate curves (pass rate vs PSD upper cutoff diameter) in the high dose variance regime (originating from high API PSD variance). Observe that the USP < 905 > pass rate curve has a steep drop to zero as the upper cutoff diameter increases for all dose strengths and that upper cutoff diameter where the drop occurs appears to be approximately logarithmic in the dose strength. These results were obtained for an API with density 1 g/cm^3 having a log-normal PSD distribution with d_{50} = 10μm and d_{90} = 100μm.

the error in the statistics computed for the dose distribution. To gain insight into the impact of the upper cutoff diameter on CU test outcomes, we investigated the dependence of simulated USP < 905 > pass rates on the upper cutoff diameter for a range of log-normal distribution parameters and target dose strengths.

In general, the USP < 905 > pass rate decreases as the PSD upper

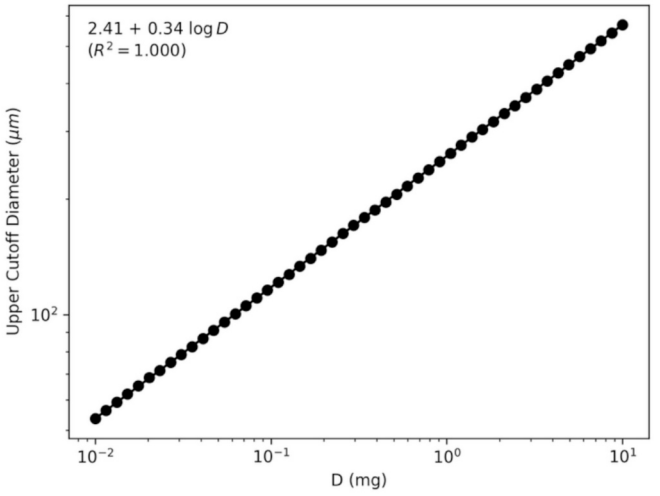

Fig. 7. In the high dose variance regime, the upper cutoff diameter (for a 95 % USP < 905 > pass rate) is proportional to a power of the dose strength with exponent slightly larger than 1/3 (indicated by the slope of 0.34 on the log–log plot). These results were obtained for an API with density 1 g/cm^3 having a log-normal PSD distribution with d_{50} = 10μm and d_{90} = 100μm.

cutoff diameter increases (Fig. 4, Fig. 5, Fig. 6, and Fig. 7). This observation is consistent with physical intuition[7] – a large upper cutoff diameter increases the probability of incorporating a large API particle into a tablet, thus increasing the probability of failing USP < 905 > . The pass rate curves can be classified into three distinct types (Fig. 4): (i) the USP < 905 > pass rate is near 100 % for all upper cutoff diameters, (ii) the USP < 905 > pass rate decreases as the upper cutoff diameter increases but is greater than zero even for very large upper cutoff diameters, and (iii) the USP < 905 > pass rate decreases and approaches zero for very large upper cutoff diameters.

The pass rate curve types are manifestations of the dose variance regimes discussed in Section 2.3.1. In the low dose variance regime (e.g., 10 mg), the variation between tablets is very low. Therefore, USP < 905 > almost never fails regardless of the upper cutoff diameter. In the medium dose variance regime (e.g., 0.5 mg and 1 mg), the variation in the API particle size leads to a wider variance in the tablet dose so that USP < 905 > does not always pass. However, the tablet dose variance is small enough that USP < 905 > always has a nonzero pass rate even if there is no upper cutoff diameter for the PSD. Finally, in the high dose variance regime (e.g., 0.1 mg), USP < 905 > always fails if the upper cutoff diameter is too large (or not imposed).

An important characteristic of the mid- and high-dose variance regimes is that the drop in the USP < 905 > pass rate curve is steep (Fig. 4), which indicates that CU simulation results are highly sensitive to the choice of upper cutoff diameter – too low a cutoff produces overly optimistic predictions while too high a cutoff leads to overly pessimistic predictions. This observation underscores the importance of selecting an appropriate API PSD upper cutoff diameter when using MC simulations to predict USP < 905 > outcomes.

Examining how the pass rate curve varies with PSD variance (Fig. 5) and dose strength (Fig. 6) provides useful insights for PSD engineering. When the dose strength is fixed (e.g., 1 mg), the pass rate curve shifts to the left as the PSD variance – which can be characterized by the ratio d_{90}/d_{50} – increases (Fig. 5). However, the pass rate curves bunch together eventually, which suggests that it should be possible to estimate (as a function of the API PSD and target dose strength) a suitable upper cutoff diameter required to achieve a desired USP < 905 > pass rate. For

[7] This intuition has long been used by formulators to reduce the risk of content uniformity test failure.

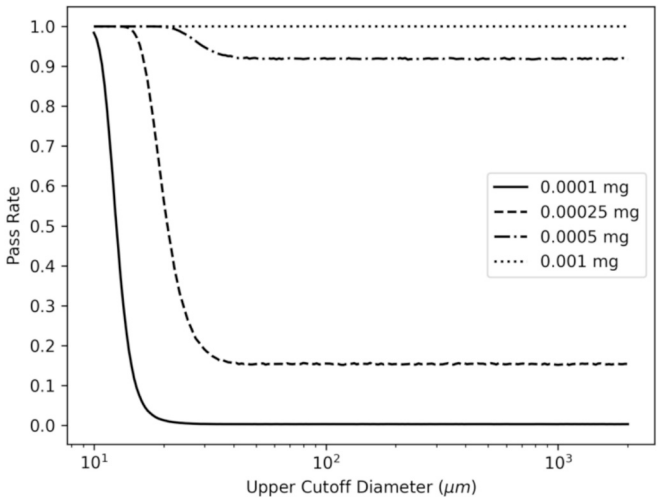

Fig. 8. Dose strength dependence of the USP < 905 > pass rate curves (pass rate vs PSD upper cutoff diameter) in the low dose variance regime (originating from low API PSD variance). Observe that difficulty passing USP < 905 > only occurs at very low dose strengths (dash and solid). At low, but not extremely low dose strengths (dot and dot-dash), USP < 905 > pass rates remain high regardless of the PSD upper cutoff diameter. These results were obtained for an API with density 1 g/cm^3 having a log-normal PSD distribution with d_{50} = 10μm and d_{90} = 15μm.

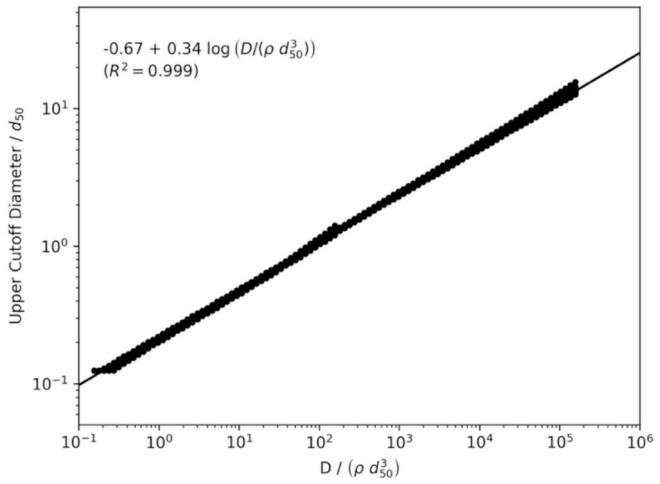

Fig. 9. Universal upper particle cutoff diameter vs dose strength curve in the high dose variance regime for APIs having a log-normal PSD. By scaling the upper particle diameter and dose as shown in the figure, the data for a range of d_{50} and d_{90} values approximately collapse onto a single line (on a log–log pot). These results were obtained for an API with density 1 g/cm^3 and a 99 % USP < 905 > pass rate.

a fixed PSD variance in the high dose variance regime, the USP < 905 > pass rate curves at different dose strengths yield a predictive relationship. The pass rate curve shifts to the right as the dose strength increases with the size of the shift proportional to a power of the dose strength with exponent slightly larger than 1/3 (Fig. 6 and Fig. 7). In contrast, when we operate in the low dose variance regime, the USP < 905 > pass rates for fixed PSD variance remains high for all upper cutoff diameters except at extremely low dose strengths (Fig. 8). Except for APIs where the particle size distribution has a very low d_{90}/d_{50} ratio (Fig. 8), sufficiently low dose strengths will result in high dose variance.

For the high dose variance regime, a universal relationship between the upper particle size cutoff and the dose strength can be found for all APIs that have an approximately log-normal particle size distribution.

Table 2
Target dose strength and (1) observed RSD values for an API with experimentally measured PSD. (2) simulated RSD values when upper cutoff diameter was set by visual inspection of the PSD.

Target Dose Strength	Observed RSD	Simulated RSD
1.0 mg	0.2316	0.24
1.5 mg	0.00533	0.02

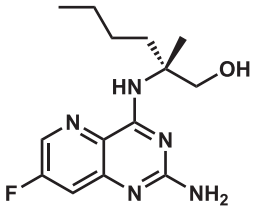

Molecular Weight: 293.35

Fig. 10. Molecular structure of selgantolimod.

Table 3
Formulation compositions (w/w %) of selgantolimod tablets at 1.0 mg and 1.5 mg dose strength.

Component	1.0 mg	1.5 mg	Source of materials
Selgantolimod	1.00	1.50	Gilead
Microcrystalline Cellulose (Avicel PH101)	61.75	61.25	FMC
Mannitol Pearlitol 100SD	31.25	31.25	Roquette
Crospovidone (Kollidon CL)	5.00	5.00	BASF SE
Magnesium Sterate	1.00	1.00	Merck
Total	100	100	

By appropriately scaling the variables, the upper cutoff diameter vs dose strength curves for different API PSD distributions approximately collapse onto a single curve (Fig. 9). Observing that $D/(\rho d_{50}^3)$ is proportional to the number of API particles contained in a tablet with dose strength D, the universal relationship tells us that the upper cutoff diameter required to achieve a desired USP < 905 > pass rate is approximately proportional to the diameter (in units of d_{50}) of a sphere formed from the average number particles contained in a single tablet.

Our study of the impact of upper cutoff diameter on USP < 905 > pass rates illustrates practical implications of our quantitative dose-regime definitions (Section 2.3). It also provides further evidence for the need to carefully choose the upper cutoff diameters in CU simulations, pointing to opportunities for PSD control strategy using early knowledge of API's properties (Section 4).

4. Simulation-based workflows for drug development and manufacturing

Using the insights gained from our theoretical analysis of the tablet formation model (Section 2) and simulation validation (Section 3), we developed principles and methods for simulation-based API PSD engineering.

4.1. Simulation design principles

4.1.1. Use empirical API PSDs whenever possible

In practice, API PSDs can deviate significantly from a log-normal distribution. Combined with the sensitivity of simulation results on the PSD upper cutoff diameter, we recommend using empirical API PSDs for simulations whenever available. To illustrate the difficulty of PSD fitting, we examine the discrepancy between simulated and empirical

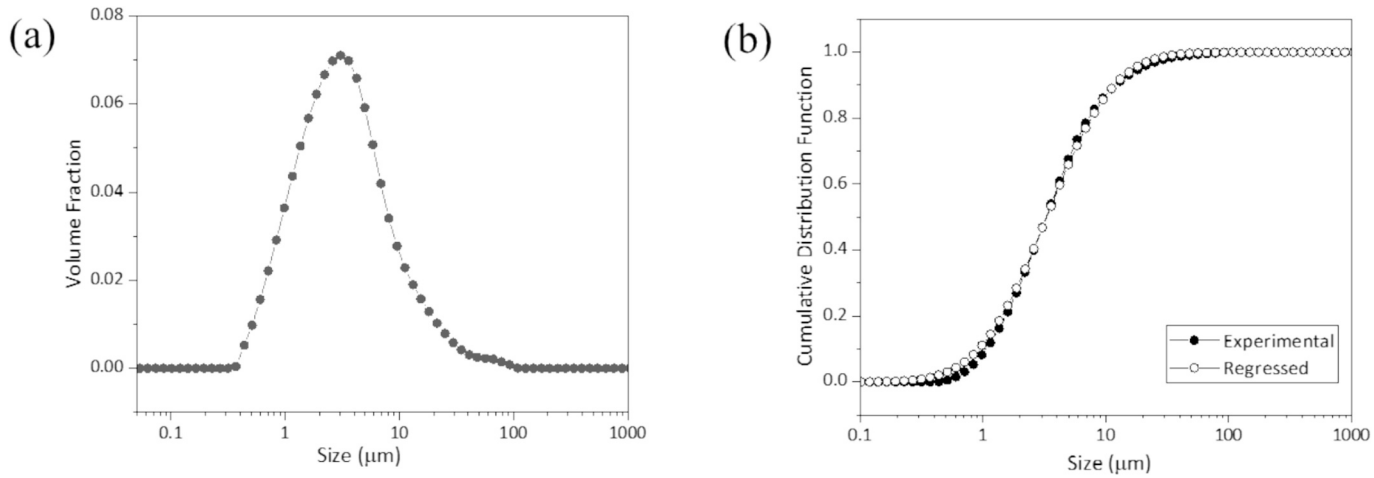

Fig. 11. (a) Experimental particle size distribution of the API by laser light scattering (b)Regression through the cumulative distribution function (CDF) of a log-normal distribution, $\mathrm{CDF}(x) = \frac{1}{2}+\frac{1}{2}\mathrm{erf}\left[\frac{\ln(x)-\ln(d_{50})}{\sqrt{2}\bullet\ln(\sigma_g)}\right]$ by the Levenberg Marquardt algorithm.

RSD for the experimental dataset in Table 2 (Observed RSD column). The experimental dataset was extracted from two batches of selgantolimod (Mackman et al., 2020; Gane et al., 2023) manufactured at 1.0 mg and 1.5 mg strength, respectively. The molecular structure of selgantolimod is shown in Fig. 10 and the composition of the formulations is summarized in Table 3.

We used the following two approaches to fit the empirical PSD. In both approaches, we first fit the empirical PSD to a log-normal distribution.

1. Set the upper cutoff diameter based on visual inspection of the maximum diameter where the empirical PSD has a nonzero density.
2. Fit the upper cutoff diameter so that the simulated RSD matches the experimental RSD for a particular target dose strength.

For the dataset, the API particle size distribution is shown in Fig. 11, and the parameters for the best fit log-normal distribution were found to be d_{50}: 3.3 μm and σ_g: 2.7.

When the PSD upper cutoff diameter was set using visual inspection of the empirical PSD, we estimated an upper cutoff diameter of 150 μm and obtained the results (Simulated RSD column) shown in Table 2.

While the simulated and experimental RSD values are reasonably close for the 1.0 mg tablets, it is about an order of magnitude too large for the 1.5 mg tablets. When we fit the PSD upper cutoff diameter using the experimental RSD value at one dose strength, there was always a discrepancy between the simulated and experimental RSD values at the other dose strength. Fitting the upper cutoff diameter to the experimental RSD for 1.0 mg tablets yielded an upper truncation diameter of 143.6 μm and an over-prediction of the RSD value for 1.5 mg tablets (simulated RSD: 0.01889, experimental RSD: 0.00533). Fitting the upper cutoff diameter to the experimental RSD for 1.5 mg tablets yielded a much smaller upper cutoff diameter of 50.7 μm but led to the opposite problem – under-prediction of the RSD value for 1.0 mg tablets (simulated RSD: 0.01889, experimental RSD: 0.00533).

4.1.2. Set the PSD upper cutoff diameter based on API processing

When empirical PSD data is unavailable, we have found the log-normal PSD useful for gaining initial insight into potential content uniformity risk but only if the PSD upper cutoff diameter is set in a physically meaningful manner. For these engineering-oriented content uniformity simulations, we recommend using a maximum particle size implied by common API processing procedure (e.g., milling and sieving). To avoid content uniformity test failures in manufacturing, we recommend setting the upper cutoff diameter conservatively to reduce

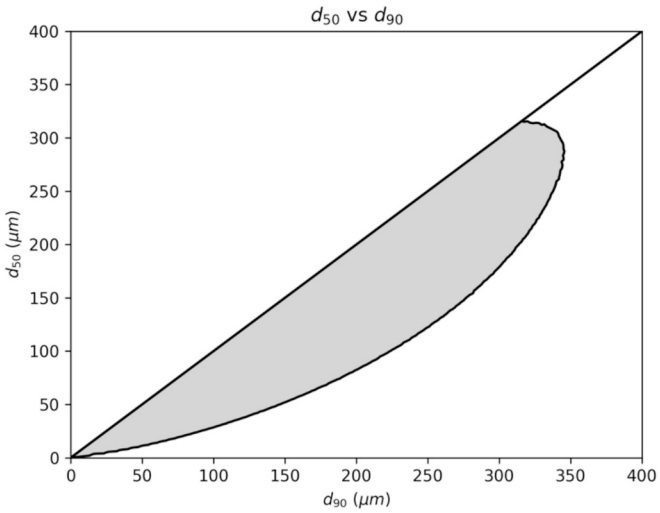

Fig. 12. Pass rate region (shaded area) for an API with density 1 g/cm^3 with a log-normal PSD truncated at 500μm when the target dose strength is $D_0 = 5$ mg and the pass rate requirement is 99%. Note that the region above the $d_{50} = d_{90}$ line cannot occur because d_{50} is never greater than d_{90}.

the likelihood that an empirical CU test fails even if the simulation predicts the content uniformity test has a high pass rate. More specifically, since large values of the upper cutoff diameter of the PSD decrease USP < 905 > pass rates, we recommend increasing the value of the upper cutoff diameter used in simulation to build a margin of safety.

4.2. From CU simulations to PSD engineering tools

To bring the power of CU simulations to process chemists and formulators, we developed a collection of PSD engineering tools (delivered as a desktop application) that support drug development workflows. These workflows provide guidance on target PSD parameters (e.g., d_{50} and d_{90}), help assess content uniformity risk, and yield deeper understanding of the distributions underlying content uniformity statistics (e.g., USP < 905 > pass rate).

4.2.1. Early-stage assessment of CU risk

Using the quantitative dose regimes defined in Section 2.3, we can assess both (1) the need for CU risk mitigation strategies and (2) whether simulations are required to accurately predict USP < 905 > failure rates

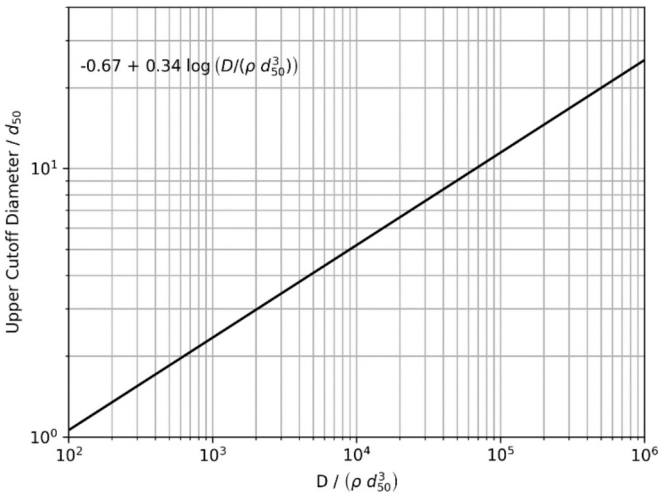

Fig. 13. The universal scaling relationship between the upper particle size cutoff and the dose strength can be used to guide selection of sieving parameters given knowledge of the target dose strength and API PSD parameters when operating in the high dose variance regime. This figure shows the particle size upper cutoff diameter needed to achieve a target USP < 905 > pass rate of 99% for an API with density 1 g/cm^3 having a log-normal PSD distribution.

stage of development, we assume that the PSD is a truncated log-normal.

For a specified upper cutoff diameter (selected with an engineering safety margin[8]), we can use simulations over a range of d_{50} and d_{90} values to identify the PSD parameters where the USP < 905 > pass rate meets our requirements (Fig. 12).

For APIs with approximately log-normal particle size distribution, we can, when operating in the high dose variance regime (Section 2.3), select a suitable upper particle size cutoff by using the relationship between target dose strengths and upper particle size cutoffs required to achieve a desired USP < 905 > pass rate (Fig. 13). Knowledge of the initial ratio of d_{90} to d_{50} (before milling or sieving) allows us to estimate the required upper particle cutoff diameter from the target dose strength or vice-versa.[9] It is worth reiterating that this predictive graph is appropriate only in the high dose variance regime – for instance, when D is less than 0.1 of the ratio in Equation (8) – and for APIs with approximately log-normal particle size distributions.

4.2.3. *Content uniformity risk assessment*

Simulations are a valuable tool in the context of content uniformity risk assessment because they provide estimates of failure rates without requiring extensive laboratory resources. Using either experimental PSD or theoretical PSD specifications, we can use simulations to predict the USP < 905 > pass rate and investigate the origin of failures. For instance, it is straightforward to extract the tablet dose distribution

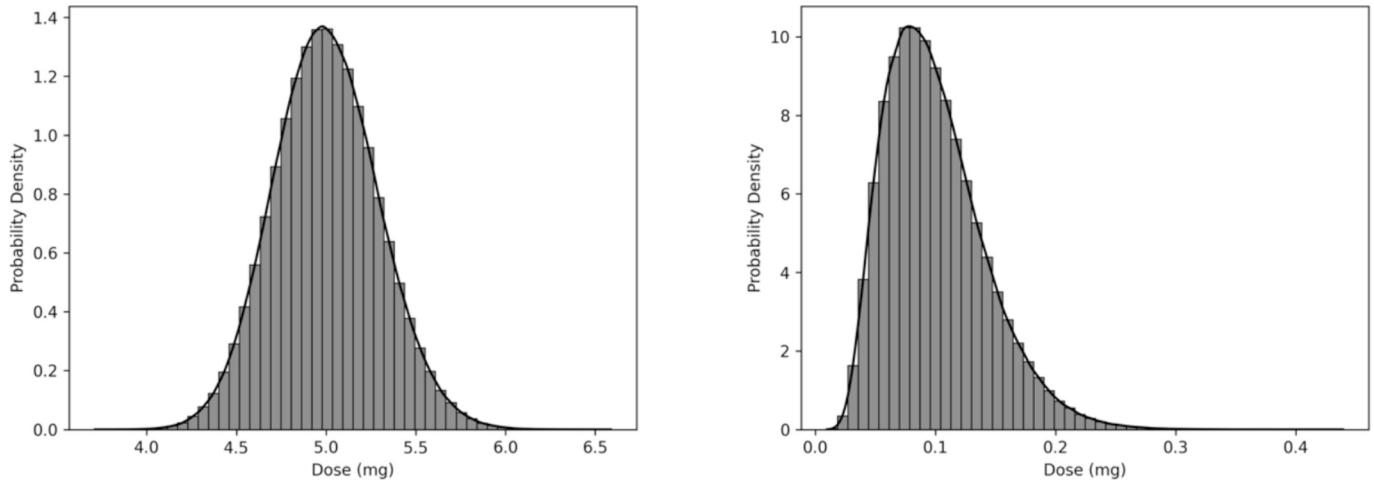

Fig. 14. Examples of tablet dose distributions constructed using data from CU simulations (Section 3). These distributions were generated for an API with density 1 g/cm^3 having a log-normal PSD distribution with d_{50} = 50 µm, d_{90} = 150 µm, and an upper cutoff of 500 µm. The figure on the left shows a low dose variance and low dose skew scenario (D_0 = 5 mg). The figure on the right shows a high dose variance and high dose skew scenario (D_0 = 0.1 mg).

(or if analytical estimates are sufficient). For example, when the API density is 1 g/cm^3 and the empirical API PSD is expected to be well-approximated by a log-normal distribution with $d_{50} = 10\mu m$ and $d_{90} = 25\mu m$, the ratio in Equation (8) is about 0.1 and the ratio in Equation (9) is about 5. If the target dose strength is $10mg$, the drug product is in the low dose variance regime (because 10 > 0.1) and low dose skew regime (because 10 > 5), so we would expect CU risk to be low.

4.2.2. *Early-stage target PSD guidance*

Even before empirical API PSD data is available, we can utilize simulations to guide API process development by providing PSD targets based on available early-stage information: API density, projected tablet dose strengths, and desired USP < 905 > pass rate. For analysis at this

(Fig. 14) and USP < 905 > acceptance value distributions (Fig. 15) from the simulations. Alternatively, for a particular API batch, we could gain insight into dose strengths that would have acceptable content uniformity failure risk (Fig. 16).

5. Conclusions

CU models and simulations can be powerful tools for process/analytical chemists and formulators, enabling them to assess content

[8] A reasonable choice for the upper cutoff diameter is any value larger than the expected maximum particle diameter after sieving.

[9] Note that the axes on the nomograph are dimensionless. The scaling for the target dose strength is chosen to give good separation between the lines for different values of d_{90}/d_{50}. Interestingly, the dimensionless target dose strength is qualitatively similar to the inverse of the square of the coefficient of variance C_v^2.

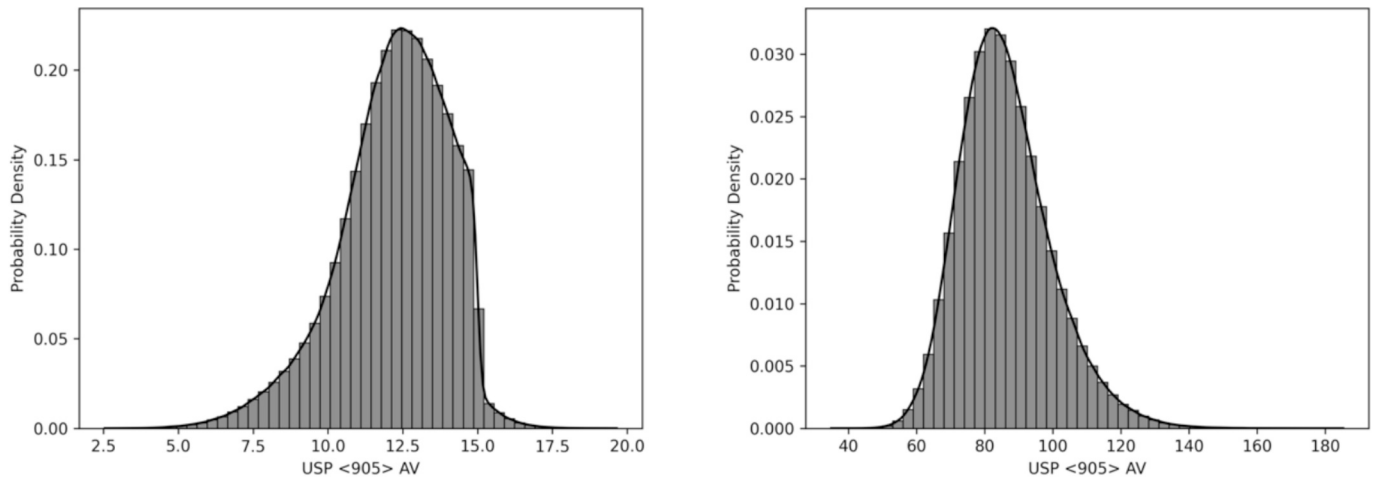

Fig. 15. Examples of USP < 905 > acceptance value (AV) distribution constructed using data from CU simulations (Section 3). This distribution was generated for an API with density 1 g/cm^3 having a log-normal PSD distribution with d_{50} = 50 μm, d_{90} = 150 μm, and an upper cutoff of 500 μm. The figure on the left shows a low dose variance and low dose skew scenario (D_0 = 5 mg). The figure on the right shows a high dose variance and high dose skew scenario (D_0 = 0.1 mg).

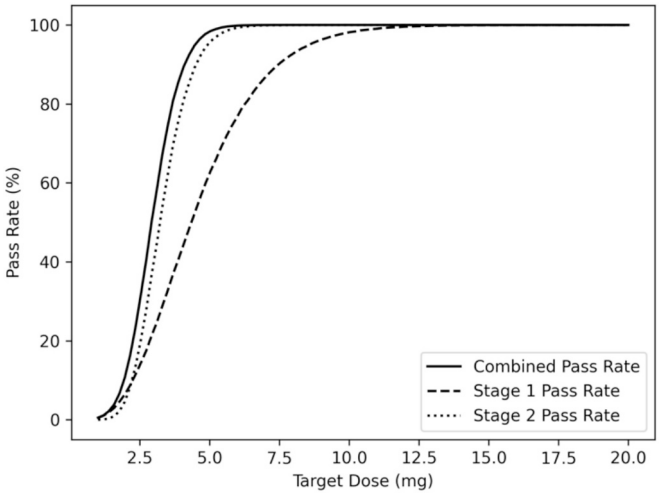

Fig. 16. Example of a USP < 905 > pass rate vs target dose strength curve based on data generated from CU simulations (Section 3). Note that the Stage 2 pass rate is conditioned on Stage 1 failing. This distribution was generated for an API with density 1 g/cm^3 having a log-normal PSD distribution with d_{50} = 50 μm, d_{90} = 150 μm, and an upper particle size cutoff of 500 μm.

uniformity risk without extensive experimental effort. However, simulations are only valuable if they are accurate, used appropriately, and embedded within natural operational workflows. With these goals in mind, we have developed quantitative characterizations of dose regimes, systematically validated a nested MC simulation (for numerical accuracy, prediction impact, and agreement with experimental data), and developed engineering guidelines and tools for process chemists and formulators.

Dose regimes facilitate early assessment of CU risk (even before running simulations). If the estimated dose regime is far outside of the CU risk range, there may be little need for concern about content uniformity, reducing the need for significant experimental or simulation effort. Note that the dose regimes are useful for both experimental PSD data and theoretical PSD models.

Our investigation of the MC simulations revealed that it is critical to appropriately set the PSD upper particle size cutoff diameter in the simulations. In all our validation studies, we found that the upper particle size cutoff diameter dramatically impacts simulation predictions. Therefore, we recommend (1) choosing upper particle size cutoff diameters based on an understanding of the maximum particle size expected from the API processing procedure and (2) increasing the simulation value to include a margin of safety.

Finally, we presented simulation-based PSD engineering and CU risk assessment tools for formulators. These tools were designed to fit into common workflows, such as early-stage guidance for PSD parameter targets, predicting USP < 905 > pass rates and statistics (either before or after experimental PSD data is available), and exploring the API PSD characteristics and dose strengths space where CU risk is low.

5.1. Future research directions

There are several research directions that could lead to further improvement of the stochastic model and MC simulation approach presented in this paper. Important aspects of tablet formation to improve include: (1) accounting for API particle morphology and (2) incorporating the impact of the excipient during tablet formation. For the former, further research is needed to develop methods to quantitatively characterize API morphology. For the latter, further research is required to develop (1) mixing and blending models and (2) quantitative characterizations of API-excipient blends. In both cases, the final step would be to integrate API morphology and API-excipient blend parameters into the the existing stochastic model for tablet formation.

CRediT authorship contribution statement

Kevin T. Chu: Writing – original draft, Software, Methodology, Investigation, Formal analysis, Conceptualization. **Remus Osan:** Writing – review & editing, Methodology, Investigation, Conceptualization. **Nicole Tin:** Writing – review & editing, Software, Methodology, Investigation, Formal analysis. **Somdatta Bhattacharya:** Writing – review & editing, Validation, Methodology, Investigation. **Chiajen Lai:** Writing – review & editing, Writing – original draft, Resources, Investigation, Formal analysis, Conceptualization.

Declaration of competing interest

The authors declare that they have no known competing financial interests or personal relationships that could have appeared to influence the work reported in this paper.

Acknowledgements

The authors would like to thank Michael Huang, Alex Kermani,

Gemma Xue, and Mandeep Chauhan for helpful discussions, Chris Regens, Ming Yang, Dazhan David Liu, and Ruby Chan for assistance obtaining experimental content uniformity data, and Victor Rucker, Chris Foti, Peter Huang, Mehul Chatrapati, and Jennifer Hedborn for their support of this work.

Appendix

A. Notation

- C_v: coefficient of variation
- d_{50}: median of particle size distribution
- d_X: X-th percentile of the particle size distribution
- D: tablet dose strength
- D_0: target dose strength
- ρ: density of material (g/cm^3)
- μ: log of the median (geometric mean) for a log-normal distribution
- σ_g: geometric standard deviation for a log-normal distribution
- Probability of event E: $P[E]$
- Expected value of random variable X: $\langle X \rangle$
- Variance of random variable X: $Var(X)$

B. Moments of the particle volume when the diameter has a Log-Normal distribution

The moments of the log-normal distribution can be computed analytically. These analytical formulas are used in the numerical convergence study (Section 3.2.1). They are also useful for estimating the dose regime when an API PSD is well approximated by a log-normal distribution.

Assuming that all particles are spheres and the diameter distribution is log-normal with parameters d_{50} and σ_g, the expected values of the first three powers of the volume V are

$$\langle V \rangle = \frac{\pi d_{50}^3}{6} \exp\left(\frac{9}{2}\log^2\sigma_g\right)$$

$$\langle V^2 \rangle = \left(\frac{\pi d_{50}^3}{6}\right)^2 \exp\left(18\log^2\sigma_g\right)$$

$$\langle V^3 \rangle = \left(\frac{\pi d_{50}^3}{6}\right)^3 \exp\left(\frac{81}{2}\log^2\sigma_g\right)$$

Data availability

Data will be made available on request.

References

Azzalini, A., 1985. A Class of Distributions which includes the Normal Ones. Scand. J. Stat. 12, 171–178.
Azzalini, A., 1986. Further results on a class of distributions which includes the normal ones. Statistica (Bologna) 46, 199–208.
Chang, M., 2010. Monte Carlo simulation for the Pharmaceutical Industry: Concepts, Algorithms, and Case Studies. CRC Press.
Gamble, J.F., Leane, M., Olusanmi, D., Tobyn, M., Supuk, E., Khoo, J., Naderi, M., 2012. Surface energy analysis as a tool to probe the surface energy characteristics of micronized materials—A comparison with inverse gas chromatography. Int. J. Pharm. 422, 238–244.
Gamble, J.F., Dawson, N., Murphy, D., Theophilus, A., Kippax, P., 2019. A Proposal for an Alternative Approach to Particle size Method Development during Early-Stage Small Molecule Pharmaceutical Development. J. Pharm. Sci. 108, 3515–3520.
Gane, E.J., Rod Dunbar, P., Brooks, A.E., Zhang, F., Chen, D., Wallin, J.J., van Buuren, N., Arora, P., Fletcher, S.P., Tan, S.K., Tang, J.C., Gaggar, A., Kottilil, S., Tang, L., 2023. Safety and efficacy of the oral TLR8 agonist selgantolimod in individuals with chronic hepatitis B under viral suppression. J. Hepatol. 78, 513–523.
Hilden, J., Schrad, M., Kuehne-Willmore, J., Sloan, J., 2012. A First-Principles Model for Prediction of Product Dose Uniformity based on Drug Substance Particle size distribution. J. Pharm. Sci. 101, 2364–2371.
Huang, C.-Y., Ku, M.S., 2010a. Prediction of drug particle size and content uniformity in low-dose solid dosage forms. Int. J. Pharm. 383, 70–80.
Huang, C.-Y., Ku, M.S., 2010b. Asymmetry effect of Particle size distribution on Content Uniformity and Over-Potency Risk in Low-Dose Solid Drugs. J. Pharm. Sci. 99, 4351–4362.
Hudson-Curtis, B., Novick, S., 2016. Chapter 24: Assessing Content Uniformity. 631-651. Nonclinical Statistics for Pharmaceutical and Biotechnology Industries. Springer International Publishing Switzerland.
Johnson, M.C.R., 1972. Particle size distribution of the active ingredient for solid dosage forms of low dosage. Pharm. Acta Helv. 47, 546–559.
Johnson, M.C.R., 1975. The effect of particle size upon mixing homogeneity. Pharm. Acta Helv. 50, 60–63.
Lachiver, E.D.R., Abatzoglou, N., Cartilier, L., Simard, J.S., 2006. Insights into the Role of Electrostatic Forces on the Behavior of Dry Pharmaceutical Particulate Systems. Pharm. Res. 23, 997–1007.
R.A. Lionberger S.L. Lee L.M. Lee A. Raw L.X. Yu Quality by design: concepts 2008 for ANDAs. AAPS Journal. 10, 268–276.
Mackman, R.L., Mish, M., Chin, G., Perry, J.K., Appleby, T., Aktoudianakis, V., Metobo, S., Pyun, P., Niu, C., Daffis, S., Yu, H., Zheng, J., Villasenor, A.G., Chamberlain, J., Jin, H., Lee, G., Suekawa-Pirrone, K., Santos, R., Delaney IV, W.E., Fletcher, S.P., 2020. Discovery of GS-9688 (Selgantolimod) as a Potent and Selective Oral Toll-like Receptor 8 Agonist for the Treatment of Chronic Hepatitis B. J. Med. Chem. 63, 10188–10203.
Martins, M.T., Lourenco, F.R., 2024. Measurement uncertainty for <905> Uniformity of Dosage units tests using Monte Carlo and bootstrapping methods – Uncertainties arising from sampling and analytical steps. J. Pharm. Biomed. Anal. 238, 115857.
Olusanmi, D., Jayawickrama, D., Bu, D., McGeorge, G., Sailes, H., Kelleher, J., Gamble, J. F., Shah, U.V., Tobyn, M., 2014. A control strategy for bioavailability enhancement by size reduction: effect of micronization conditions on the bulk, surface and blending characteristics of an active pharmaceutical ingredient. Powder Technol. 258, 222–233.
Parikh, R.B., Obermeyer, Z., Navathe, A.S., 2021. Regulation of predictive analytics in medicine. Science 363, 810–812.
Park, J.-B., Kang, C.-Y., Kang, W.-S., Choi, H.-G., Han, H.-K., Lee, B.-J., 2013. New investigation of distribution imaging and content uniformity of very low dos drugs using hot-melt extrusion method. Int. J. Pharm. 458, 245–253.
Pinsky, M.A., Karlin, S., 2011. *An Introduction to Stochastic Modeling*, 4th edition,. Elsevier.
Rhodes, M., Seville, J., 2024. *Introduction to Particle Technology*. John Wiley & Sons Ltd.

Rohrs, B.R., Amidon, G.E., Meury, R.H., Secreast, P.J., King, H.M., Skoug, C.J., 2006. Particle size Limits to Meet USP Content Uniformity Criteria for Tablets and Capsules. Pharmaceutical Sciences 95, 1049–1059.
Saravanan, D., Muthudoss, P., Khullar, P., Rose, V.A., 2021. Micronization and Agglomeration: Understanding the Impact of API Particle Properties on Dissolution and Permeability using Solid State and Biopharmaceutical "Toolbox". J. Pharm. Innov. 16, 136–151.
Schulze, D., 2021. Powders and Bulk Solids - Behavior, Characterization, Storage and Flow, 2nd edition,. Springer.
Seibert, K., Collins, P.C., Luciani, C.V., 2019. Chapter 38: Milling operation in the Pharmaceutical Industry. 861-879. Chemical Engineering in the Pharmaceutical Industry: Active Pharmaceutical Ingredients, 2nd Ed. Wiley.
United States Pharmacopeia, 2023. *General Chapter, ⟨905⟩ Uniformity of Dosage units*. United States Pharmacopeia, USP-NF. Rockville, MD.
Wang, Y., Zhu, H., Madabushi, R., Liu, Q., Huang, S.-M., Zineh, I., 2019. Model-Informed Drug Development: Current US Regulatory Practice and Future Considerations. Clin. Pharmacol. Ther. 105, 899–911.
Yalkowsky, S.H., Bolton, S., 1990. Particle size and content uniformity. Pharm. Res. 7, 663–676.
Yu, L.X., 2008. Pharmaceutical Quality by Design: product and Process Development. Understanding, and Control, Pharmaceutical Research 25, 781–791.
Zhang, Y., Johnson, K.C., 1997. Effect of drug particle size on content uniformity of low-dose solid dosage forms. Int. J. Pharm. 154, 179–183.
Zheng, J. (Ed.), 2009. Formulation and Analytical Development for Low-Dose Oral Drug Products. Wiley, New Jersey.